Trapping-Induced Enhancement of Photocatalytic Activity on Brookite TiO2 Powders: Comparison with Anatase and Rutile TiO2 Powders

a

Journal:	*ACS Catalysis*
Manuscript ID	Draft
Manuscript Type:	Article
Date Submitted by the Author:	n/a
Complete List of Authors:	

Trapping-Induced Enhancement of Photocatalytic Activity on Brookite TiO_2 Powders: Comparison with Anatase and Rutile TiO_2 Powders

Junie Jhon M. Vequizo,[a] *Hironori Matsunaga,*[a] *Tatsuya Ishiku,*[b] *Sunao Kamimura,*[b] *Teruhisa Ohno,*[*b] *and Akira Yamakata*[*c]

a Graduate School of Engineering, Toyota Technological Institute, 2-12-1 Hisakata, Tempaku, Nagoya 468-8511, Japan

b Department of Materials Science, Faculty of Engineering, Kyushu Institute of Technology, 1-1 Sensui-cho, Tobata-ku, Kitakyushu, Fukuoka, 804-8550, Japan

c Precursory Research for Embryonic Science and Technology (PRESTO), Japan Science and Technology Agency (JST), 4-1-8 Honcho Kawaguchi, Saitama 332-0012, Japan

Abstract: Brookite TiO_2 is a promising material for active photocatalysts. However, the principal difference in the behavior of photogenerated electrons and holes in brookite TiO_2 compared to that in anatase and rutile TiO_2 has not yet been fully elucidated. In this work, we studied the behavior of photogenerated electrons and holes in several TiO_2 powders by using femtosecond to millisecond time-resolved visible to mid-IR absorption spectroscopy. We found that most of the free electrons are trapped at powder defects within a few ps. This electron trapping decreases the number of surviving free electrons, but extends the lifetime of holes as well as the trapped electrons since the mobility of electrons decreases. The number of surviving holes is increased; therefore the electron trapping enhances the photocatalytic oxidation. On the contrarily, the reactivity of electrons is decreased to some extent by trapping, but they remain reactive with O_2. Electron trapping also takes place on anatase and rutile TiO_2 powders, but the trap-depth is too shallow to extend the lifetime of holes in anatase and too deep for an effective electron-consuming reaction on rutile TiO_2, respectively. The moderate depth of the electron trap in brookite TiO_2 maintains reactivity with O_2 while extending the lifetime of holes. As a result, both of electrons and holes are reactive. These results clearly demonstrate that appropriate depth of the electron trap can positively work to enhance the overall photocatalytic activity.

TOC GRAPHICS

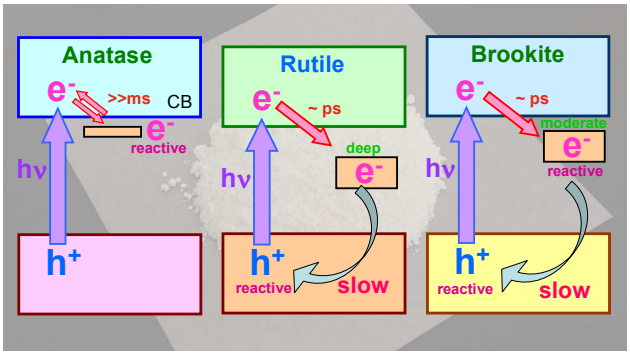

KEYWORDS: TiO_2 photocatalysts, photogenerated charge carriers, surface-defects, charge trapping, recombination, time-resolved absorption spectroscopy.

1. Introduction

Photocatalysts attract considerable interest due to their potential applications for water-splitting reaction and degradation of pollutants by using solar energy. TiO_2 is one of the most widely used materials for photocatalysis, primarily because of its abundance and chemical stability. [1-5] There are three polymorphs in the crystal structure of TiO_2: anatase, rutile, and brookite. The photocatalytic activity of anatase and rutile TiO_2 has been well studied; however there have been relatively much fewer studies on brookite TiO_2 because the synthesis of pure brookite powder is technically difficult. However, the recent development of an improved synthesis method has prompted more studies of brookite TiO_2, which is now attracting considerable attention for application not only to photocatalysts[6-15] but also to perovskite solar cells:[16] Brookite TiO_2 demonstrates superior performance for several photocatalytic reactions than anatase and rutile TiO_2.[6-15] Despite of these promising reports on brookite TiO_2, the reason why brookite TiO_2 has higher activity is not fully elucidated yet. Photocatalytic activity is determined by the behavior of photogenerated electrons and holes, but as far as we know, the photodynamical processes on brookite TiO_2 powders have not yet been reported. For the further use of TiO_2 as a light-energy conversion material, the differences in the photodynamical processes among anatase, rutile, and brookite should be elucidated.

Time-resolved absorption spectroscopy is useful to study the behavior of photogenerated charge carriers on photocatalysts. This method has been applied to investigate the differences in photocatalytic activity between anatase and rutile TiO_2. [17-24] In the case of single-crystalline TiO_2, it is established that the electron-hole pair recombination is faster in rutile than in anatase. [25-26] However, recently we found that the results are opposite in the case of powder: the recombination is slower in rutile than in anatase.[24] This discrepancy comes from the electron-

trapping at the defects, which are rich on powder particles. Most of the free electrons in rutile TiO_2 are deeply trapped within a few ps,[24] which then decrease the probability of electron to encounter with holes. As a result, the lifetime of holes becomes longer and thus enhances the photocatalytic oxidation reactions. In the case of anatase TiO_2 powders, the depth of the electron-trap is shallower, so the reactivity of electrons is higher.[24] However, the lifetime of holes is shorter than that in rutile. These are the reasons why anatase and rutile TiO_2 exhibit distinct photocatalytic activities: anatase shows higher activity for reduction but rutile shows higher activity for oxidation. These results confirm us that the electron-trapping at the powder defects positively works in elongating the lifetime of charge carriers, but too deep trapping negatively works to decrease their reactivity. The trap-depth governs the overall photocatalytic activity.

In this work, we examined the behavior of photogenerated charge carriers at the defects on brookite TiO_2 powders by using time-resolved absorption spectroscopy. Two different brookite TiO_2 powders, as-synthesized fine crystals[7, 15] and a commercial powder (Kojundo Chemicals, Ltd.) were investigated. We found that the depth of the electron-trap on TiO_2 powders is not so sensitive to the morphology of the powder particles, but strongly depends on the crystal structure of TiO_2. Brookite TiO_2 powders have moderate depth of the electron-trap compared to anatase and rutile TiO_2 powders, therefore the lifetime of holes in brookite are longer than in anatase and the trapped electrons are reactive than those in rutile TiO_2 powders. Based on these behaviors of photogenerated electrons and holes, the principal mechanism that determines the distinctive activity of brookite TiO_2 powders has been discussed.

2. Experimental

"As-synthesized" brookite TiO_2 was prepared by hydrothermal synthesis method as reported previously by one of our co-authors (Ohno et al). [15] Briefly, a 12.5 mmol amorphous titanium hydroxide particles dispersed in 40 mL H_2O_2 (30%) were used as starting precursors and then 10 mL ammonia and glycolic acid were added. The mixture solution was stirred for 6 h at constant temperature of 60^{o}C, after which an orange-colored gel compound was obtained. The gel was then dispersed in deionized water and the pH was adjusted to 10 by adding ammonia. The volume of the solution was adjusted using deionized water until it reached 50 mL and this final mixture solution undergone hydrothermal treatment at 200^{o}C for 48 h. After the treatment, the residue was washed with deionized water and dried under reduced pressure at 60^{o}C for 12 h. On the other hand, "commercial" brookite TiO_2 powders purchased from Kojundo Chemical Ltd was used as-received. Anatase (TIO-1) and Rutile (TIO-3) TiO_2 powders supplied by the Catalysis Society of Japan[24] were also used for the comparison. Prior to time-resolved absorption spectroscopic measurements, two brookite TiO_2 powders, commercial-brookite (specific surface area: 22.7 m^2/g) and synthesized-brookite (specific surface area: 45 m^2/g) [15], were prepared separately on CaF_2 plate with density of 3 mg cm^{-1} and used without further treatments. Then, these samples were placed in a tightly closed sample cell.

The microsecond time-resolved visible to mid-IR absorption measurements were performed by using the laboratory-built spectrometers as described in our previous papers. [27] Briefly, in the mid-IR region (6000 ~ 1000 cm^{-1}), the measurement was carried out in transmission mode, wherein the probe light emitted from a $MoSi_2$ coil was focused on the sample and then the transmitted light was introduced to the grating spectrometer. The monochromated light was then detected by an MCT detector (Kolmar) and the output electric signal was amplified with AC-coupled amplifier (Stanford Research Systems, SR560, 1 MHz). In the

visible to NIR region (25000 ~ 6000 cm^{-1}), the experiments were performed in the reflection mode, wherein the probe light that comes from the halogen lamp (50 W) was focused on the sample and detected using Si or InGaAs photodiodes. In each experiment, the pump UV (355 nm) laser pulses that originated from a Nd:YAG laser (Continuum, Surelite I, duration: 6 ns, power: 0.5 mJ, repetition rate: 10~0.01 Hz) were utilized to excite the photocarriers of brookite TiO_2 samples. The time resolution of the spectrometers was limited to 1 ~ 2 μs by the bandwidth of the amplifier. To determine the decay processes and reactivity of photogenerated charge carriers, the measurements were performed in vacuum, or in the presence of 20 Torr O_2 gas or MeOH vapor at room temperature. [23, 28]

Femtosecond time-resolved visible to mid-IR absorption measurements were performed by utilizing a pump-probe technique based on femtosecond Ti:Sapphire laser system (Spectra Physics, Solstice & TOPAS prime, duration: 90 fs, repetition rate: 1 kHz) as described in our previous paper. [27] In this experiment, a 350-nm pulse was utilized for excitation of the photocatalysts, and 22000 cm^{-1} (455 nm), 14300 cm^{-1} (700 nm), and 2000 cm^{-1} (5 μm) pulses were used for the probe light. In the mid-IR region, the probe light transmitted from the sample was detected by an MCT array detector (Infrared Systems Development Corporation, 128 Ch, 6000~1000 cm^{-1}). On the other hand, in the visible to NIR region, the diffuse reflected probe light was detected by photomultiplier (Hamamatsu Photonics, H5784-03, 25000 ~ 14300 cm^{-1}). The detection of the NIR is limited only up to 14300 cm^{-1} by the sensitivity of the photomultiplier.

The PL spectra of brookite, anatase, and rutile TiO_2 powders were measured at room temperature in air. Prior to the PL measurement, the TiO_2 powders were prepared on a circular disk and placed vertically in a sample cell. A 375 nm laser photodiode with a power of 6.5 mW

(Toptica Photonics, iBeam smart) was focused on the sample and used to excite the band gap of the photocatalysts. The spectra of the emitted light were then detected using the CCD camera (Princeton Instruments, PIXIS:100F) coupled to the grating spectrometer (Acton, SP2300).

3. Results and Discussion

3.1 Transient Absorption Spectra of Brookite TiO_2 powders

We first measured the transient absorption (TA) spectra of as-synthesized brookite TiO_2 powders. These particles were prepared by hydrothermal synthesis, as reported previously.[7, 15] Fine crystals were obtained, as shown in Figure S1, and characteristic peaks of brookite crystal were observed in the XRD pattern (Figure S2). A TA spectra measured after 355 nm laser pulse irradiation (6 ns duration, 5 Hz, 0.5 mJ cm^{-2}) is shown in Figure 1a. A broad absorption was observed over the entire wavenumber region from 25000 to 3000 cm^{-1} (400 nm to 2.5 μm). Two broad absorption peaks appeared at 22000 and 13000 cm^{-1}, and these were both assigned to deeply trapped electrons, as will be discussed later. There was very little absorption below 3000 cm^{-1}. As free electrons give a strong absorption below 3000 cm^{-1}, this result suggests that most of the electrons were deeply trapped at defects, and the number of surviving free electrons was very small.

In order to understand the general features of brookite TiO_2 powders, another powder, purchased from Kojundo-Chemicals, Ltd., was examined. The obtained SEM image (Figure S1) shows that small particles aggregated to form larger secondary particles (around a few μm). The TA spectrum of the commercial powder (Figure 1b) is similar to that of as-synthesized brookite TiO_2 powders (Figure 1a), in which the absorption intensity below 3000 cm^{-1} is much weaker than that at 25000-3000 cm^{-1} although the absorption intensity around 22000 cm^{-1} is lower.

These results confirm that most of the photogenerated electrons in brookite TiO_2 powders are deeply trapped at defects. The depth of the electron trap can be estimated from the absorption edge of the deeply trapped electrons. In the case of as-synthesized brookite TiO_2 powders, the absorption edge is positioned at ~3000 cm^{-1} (~0.4 eV), so the depth was estimated to be ~0.4 eV. This value is similar to that of commercial brookite TiO_2 powders, for which the absorption edge is located at ~3000 cm^{-1}. These results suggest that the depth of the electron trap is similar for all brookite TiO_2 powders, and is not very sensitive to the morphology or particle size of the powder.

Similarly shaped transient absorption spectra to those of brookite TiO_2 powders were observed for rutile TiO_2 powders (Figure 1c, TIO-3 supplied by Catalysis Society of Japan). In these spectra, the absorption intensity of deeply trapped electrons is higher than that of free electrons. In the case of rutile TiO_2 powders, the depth of the electron trap was estimated to be ~0.9 eV[24] from the absorption edge at ~7000 cm^{-1} (~0.9 eV). This result is in contrast to that of anatase TiO_2 particles (Figure 1d, TIO-3 supplied by Catalysis Society of Japan), for which the intensity of free electrons (<3000 cm^{-1}) is much larger than that of deeply trapped electrons (> 7000 cm^{-1}). In this case, the electron trap is shallower than 0.1 eV because the absorption edge was not observed until

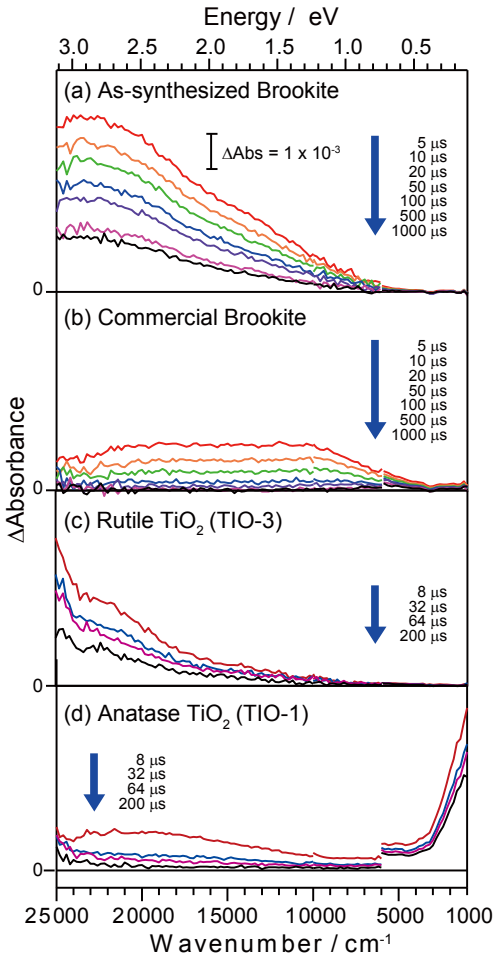

Figure 1. Transient absorption spectra of (a) as-synthesized brookite TiO_2 powder and (b) commercial brookite TiO_2 powder excited by UV laser pulses (355 nm, 6 ns duration, 0.5 mJ per pulse, and 5 Hz) in vacuum. Also shown are transient absorption spectra of rutile (c) and anatase TiO_2 powders (d) after band gap excitation.

1000 cm^{-1}. [24] These results indicate that the electron traps in TiO_2 powders grow deeper in the order: rutile > brookite > anatase.

3.2 Behavior of photogenerated charge carriers in the presence and absence of reactant molecules

The decay processes of transient absorption in as-synthesized brookite TiO_2 particles were further examined in the presence and absence of reactant molecules. As shown in Figure 2a, the intensity at 2000 cm^{-1} decreased within 2 μs of exposure to O_2 gas. This result suggests that the absorption at 2000 cm^{-1} reflects the number of electrons present, since adsorbed O_2 consumes electrons and accelerates electron decay.[23] However, exposure to MeOH vapor increased the absorption intensity, indicating that holes are consumed by MeOH, and the hole-consuming reaction prevents recombination and extends the lifetime of electrons.[28] The absorption intensities at 13000 cm^{-1} and 22000 cm^{-1} behaved similarly to that at 2000 cm^{-1} (Figure 2b and 2c, respectively), although the intensity was relatively unchanged by the O_2 exposure. These results confirm that these absorptions reflect the number of electrons, i.e., the broad absorption from 25000–1000 cm^{-1} in Figure 1a reflects the number of trapped electrons.

In the commercial brookite TiO_2 powders, the absorption intensity at 2000 cm^{-1} also reflects the number of free electrons, as shown in Figure S3. However, the absorption intensities at 22000 cm^{-1} and 13000 cm^{-1} reflect the number of both electrons and holes, as the intensity was increased by exposure to both O_2 and MeOH. This result initially seems confusing but as we reported previously,[29] if a particular absorption reflects the number of both electrons and holes, then the intensity will increase when either an electron- or hole-consuming reaction takes place.

These results demonstrate that the trapped holes provide an absorption band at 25000–7000 cm^{-1} for commercial brookite TiO_2 powders. For as-synthesized brookite TiO_2, no absorption of holes was observed from 25000–3000 cm^{-1}. These results suggest that the holes are deeply trapped in the commercial powders, but not in the as-synthesized powders. It is often proposed that the surface OH groups and surface lattice oxygen species work as hole-trapping sites, and they are readily formed on rough surfaces.[3-4] In the case of bulk single crystals such as $SrTiO_3$,[30] the absorption of trapped holes is absent from the visible region. Therefore, similar results can be expected for fine single-crystal brookite TiO_2 particles: the difference in the appearance of the trapped hole signal arises from the difference in surface morphology between as-synthesized and commercial brookite TiO_2 powders. The former is very smooth but the latter is very rough, as shown in Figure S1.

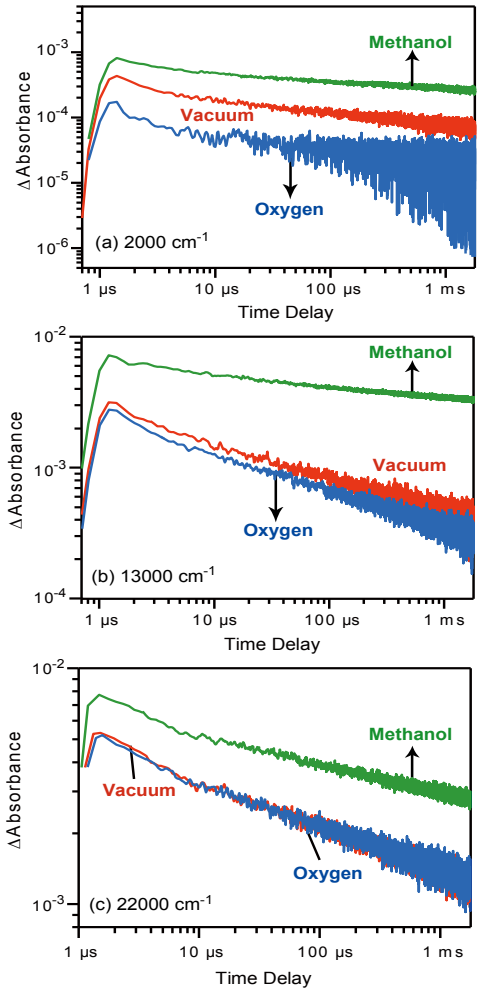

Figure 2. Decay curves of transient absorption of as-synthesized brookite TiO_2 powder irradiated by UV laser pulses (355 nm and 0.5 mJ per pulse) probed at 2000 cm^{-1} (a), 13000 cm^{-1} (b), and 22000 cm^{-1} (c) in vacuum, 20 Torr O_2, and CH_3OH.

3.3 Deep electron trapping at defects in brookite TiO_2 powders

In order to further examine the electron trapping process, the decay processes in the picosecond region were further studied using femtosecond laser systems. The normalized decay curves measured at 2000, 14300 (700

nm), and 22000 (455 nm) cm^{-1} are shown in Figure 3. As shown in the figure, the rate of decay of free electrons (2000 cm^{-1}) is much faster than that of deeply trapped electrons (22000 cm^{-1} and 14300 cm^{-1}) at 0–800 ps. This indicates that the free electrons are deeply trapped at 0~800 ps. The initial decay processes at 0–12 ps (inset figure) provide more detailed information: the number of free electrons increases within 0.5 ps, but rapidly decreases from 0.5–2 ps. On the other hand, the number of deeply trapped electrons (14300 and 22000 cm^{-1}) increases more slowly, and it takes ~2 ps to reach the maximum. The decrease in free electrons and increase in deeply trapped electrons are well correlated, suggesting that most of the free electrons excited in the CB are trapped within a few ps. As a result, the number of surviving electrons at 2000 ps is larger in the order of deeply trapped electrons (22000 cm^{-1}) > trapped electrons (14300 cm^{-1}) > free electrons (2000 cm^{-1}). This order is consistent with observations of the microsecond region (Figure 1a), where the intensity at 22000 cm^{-1} is larger than those at 14300 cm^{-1} and 2000 cm^{-1}. This confirms that the rate of decay of deeply trapped electrons is much slower than that of free electrons, and the number of carriers surviving in the microsecond region is determined by the ps-scale dynamics.

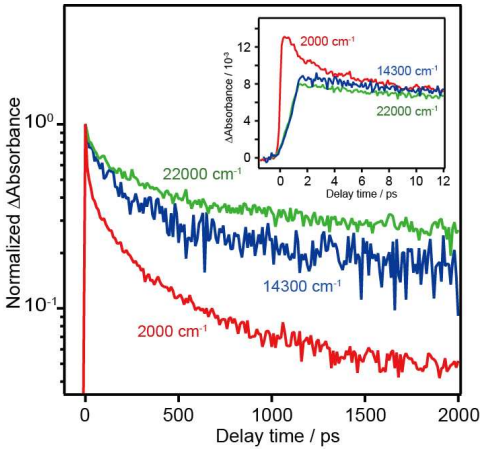

Figure 3. Decay curves of free electrons (2000 cm^{-1}) and deeply trapped electrons (14300 and 22000 cm^{-1}) in as-synthesized brookite TiO_2 powders measured by UV laser pulse irradiation (350 nm and 6 μJ per pulse, 500 Hz) in vacuum.

Similar results were observed for commercial brookite TiO_2 powders (Figure S4): the decay of free electrons is much faster than those of deeply trapped electrons and holes, giving absorption bands at 14300 and 22000 cm^{-1}. These results confirm that the electron-deep trapping

process was not sensitive to the differences in particle size and surface morphology. This rapid electron-trapping is also observed in rutile TiO_2 powders, but not in anatase TiO_2 powders, as reported in our previous paper.[24]

3.4 Photoluminescence spectra of brookite TiO_2 powders

Photoluminescence (PL) measurements provide useful information about the trapping states of charge carriers, and hence have been widely applied for many photocatalysts such as anatase and rutile TiO_2. [31-34] In this work, we measured PL spectra using a diode laser (375 nm, 6.5 mW) and a CCD camera. The results are shown in Figure 4. A strong emission peak appeared at 850 nm when as-synthesized brookite TiO_2 powders were irradiated by UV light. A similar NIR emission is observed for commercial brookite TiO_2 powders, although the intensity is much lower. An additional weak emission was observed at 590 nm, and was assigned to the radiative recombination of shallowly trapped electrons and holes.[35] The NIR emission was assigned to the radiative recombination of deeply trapped charge carriers, as the red-shift of the emission peak

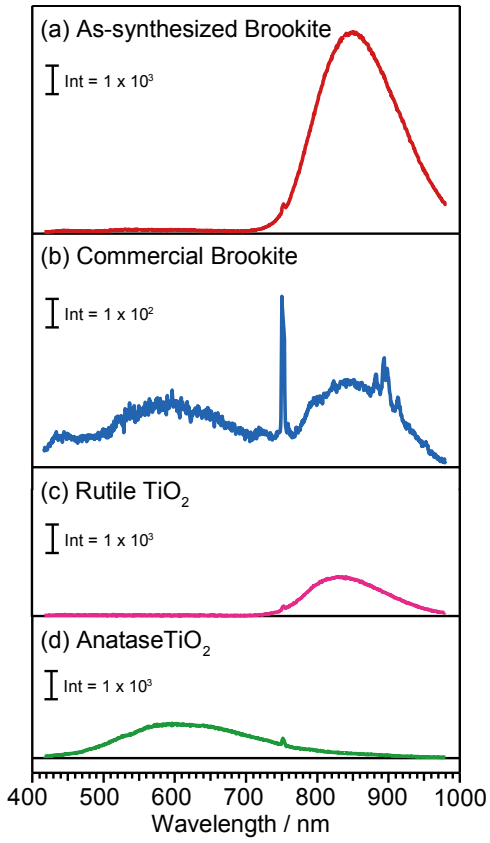

Figure 4. Photoluminescence spectra of (a) as-synthesized brookite TiO_2 powder, (b) commercial brookite TiO_2 powder excited by UV laser (375 nm, 6.5 mW) in air. PL spectra of rutile TiO_2 powder (TIO-3) and anatase TiO_2 powder (TIO-1) are shown in (c) and (d), respectively. The small signal at 750 nm is an artifact that comes from the UV laser.

into the NIR region suggests that either electrons or holes are deeply trapped in the mid-gap states with losing their energies.

From PL measurements only, it is difficult to identify whether electrons or holes are deeply trapped. However, considering the TA spectra shown in Figure 1, it is clear that the electrons are deeply trapped. Similar results and conclusions were derived for rutile TiO_2 powders, where an NIR emission is observed at 840 nm (Figure 4c) and most of the electrons are deeply trapped within a few ps.[24] In anatase TiO_2 powders, the lifetime of free and shallowly trapped electrons is longer than 1 ms[24] and the NIR emission is absent (Figure 4d). We obtained consistent results among TA and PL spectra for anatase, rutile, and brookite TiO_2 powders.

It is often reported that the origin of the electron trap is a defect such as an oxygen vacancy or Ti-interstitial.[36-38] The depth of the electron trap depends on how the defects stabilize the trapped electrons through structural relaxation (polaron formation).[36-38] In other words, as the lattice of a particle becomes more deformed, the trapped electrons become increasingly stabilized. Theoretical calculations predicted stabilization energies of 0.8–1 eV and 0–0.2 eV for rutile and anatase, respectively. [36, 38] For brookite TiO_2, we could not find any theoretical papers describing polaron formation, but oxygen vacancies and Ti-interstitials should result in similar electron traps. We estimated the depth of the electron trap to be ~0.4 eV from the absorption edge of the transient absorption at ~3000 cm^{-1} (~0.4 eV), which is deeper than that of anatase (<0.1 eV) but shallower than that of rutile (~0.9 eV), as described in the previous section.

3.5 Photocatalytic activity of brookite TiO_2: Differences from anatase and rutile TiO_2

The decay processes of photogenerated charge carriers in brookite TiO_2 powders were compared with those in anatase and rutile TiO_2 powders. As shown in Figure 5a, free electrons (2000 cm^{-1}) in both brookite TiO_2 powders decayed faster than in anatase, but slower than in rutile TiO_2. As a result, the number of surviving free electrons in the microsecond region decreases in the order: anatase > brookite > rutile. On the contrary, the trapped electrons responsible for the absorptions at 13000 cm^{-1} (Figure 5b) and 22000 cm^{-1} (Figure 5c) in as-synthesized brookite TiO_2 have longer lifetimes than those in anatase, rutile, and commercial brookite TiO_2. These results indicate that the lifetime of holes is longest in as-synthesized brookite, because the same number of holes and trapped electrons should survive to maintain charge balance, although we could not directly observe the number of free holes.

The photocatalytic activity of the as-synthesized brookite TiO_2 was reported to have a higher activity for acetaldehyde oxidation than anatase or commercial brookite TiO_2 powder.[7] These results suggest that photocatalytic activity is well correlated with the number of surviving holes rather than free electrons. Since holes usually have sufficient energy to oxidize many reactants, and because the hole-consuming

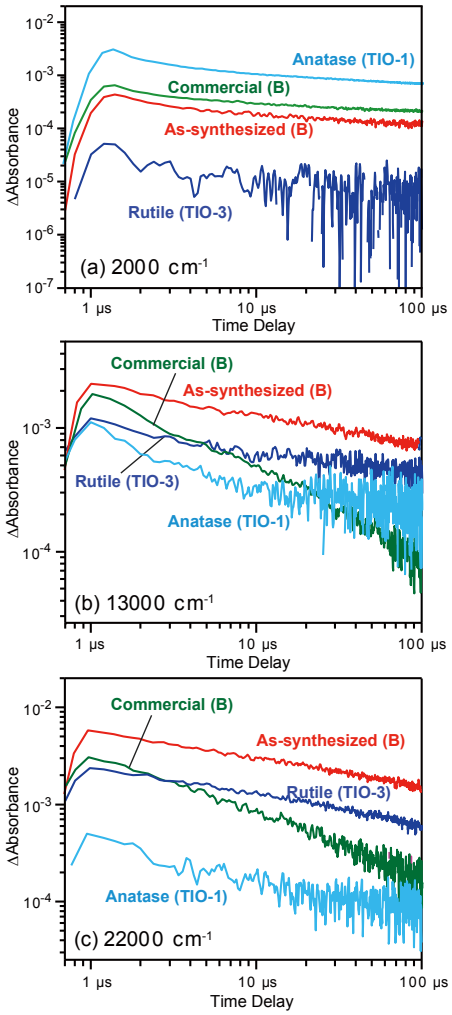

Figure 5 Decay curves of transient absorption measured at (a) 2000, (b) 13000, and (c) 22000 cm^{-1} in vacuum. As-synthesized and commercial brookite, anatase (TIO-10), and rutile (TIO-6) TiO_2 powders were irradiated by UV laser pulses (355 nm, 6 ns duration, and 0.5 mJ per pulse).

reactions proceed much faster than electron-consuming reactions,[23 28] increasing the number of surviving holes has a direct positive effect on photocatalytic oxidation. However, under steady-state reaction conditions, the activity of photocatalytic oxidation is not always solely determined by the number of surviving holes. The reactivity of electrons is also important because without electron-consuming reactions, the electrons are over accumulated in the particles and then shorten the lifetime of holes. In the case of rutile TiO_2, the lifetime of holes is longer than in anatase but the reactivity of electrons is very low: the electron trap in rutile (~0.9 eV) is deeper than in brookite (~0.4 eV) and anatase (<0.1 eV). Furthermore, the conduction band of rutile is lower than those of anatase and brookite, so rutile does not have a higher activity in many photocatalytic reactions. In the case of brookite TiO_2, both trapped electrons and holes have a reasonable reactivity, so brookite is expected to have a higher activity than anatase and rutile TiO_2 powders.

4. Conclusion

In this work, we found that brookite TiO_2 powders have moderate depth of the electron-trap that can promote both of photocatalytic oxidations and reductions. Electron-trapping at powder defects retards electron-hole recombination. The depth on rutile is too deep for electron-induced reductions, but that on anatase is too shallow to elongate the lifetime of holes. Powder defects work positively and negatively on the lifetime and reactivity of charge carriers, respectively, and hence appropriate depth is necessary to maximize the photocatalytic activity.

ASSOCIATED CONTENT

Supporting Information. XRD patterns, SEM images, Decay curves for commercial brookite TiO_2. "This material is available free of charge via the Internet at http://pubs.acs.org."

AUTHOR INFORMATION

Corresponding Author

*Akira Yamakata, E-mail: yamakata@toyota-ti.ac.jp

*Teruhisa Ohno, Email: tohno@che.kyutech.ac.jp

Notes

The authors declare no competing financial interests.

ACKNOWLEDGMENT

This work was supported by the PRESTO/JST program "Chemical Conversion of Light Energy", the Grant-in-Aid for Basic Research (B) (No. 16H04188) and Scientific Research on Innovative Areas (Area 2503; No. 16H00852), and the Strategic Research Infrastructure Project of MEXT.

REFERENCES

(1) Fujishima, A.; Honda, K. *Nature* **1972**, *238*, 37-38.

(2) Kamat, P. V. *Chem. Rev.* **1993**, *93*, 267-300.

(3) Linsebigler, A. L.; Lu, G. Q.; Yates, J. T. *Chem. Rev.* **1995**, *95*, 735-758.

(4) Hoffmann, M. R.; Martin, S. T.; Choi, W. Y.; Bahnemann, D. W. *Chem. Rev.* **1995**, *95*, 69-96.

(5) Ma, Y.; Wang, X.; Jia, Y.; Chen, X.; Han, H.; Li, C. *Chem. Rev.* **2014**, *114*, 9987-10043.

(6) Ohtani, B.; Handa, J.; Nishimoto, S.; Kagiya, T. *Chem. Phys. Lett.* **1985**, *120*, 292-294.

(7) Murakami, N.; Kamai, T.-a.; Tsubota, T.; Ohno, T. *Catalysis Communications* **2009**, *10*, 963-966.

(8) Augugliaro, V.; Loddo, V.; Lopez-Munoz, M. J.; Marquez-Alvarez, C.; Palmisano, G.; Palmisano, L.; Yurdakal, S. *Photochem Photobiol Sci* **2009**, 663-669.

(9) Kandiel, T. A.; Feldhoff, A.; Robben, L.; Dillert, R.; Bahnemann, D. W. *Chem. Mat.* **2010**, *22*, 2050-2060.

(10) Magne, C.; Cassaignon, S.; Lancel, G.; Pauporte, T. *Chemphyschem* **2011**, *12*, 2461-2467.

(11) Zhang, L.; Menendez-Flores, V. M.; Murakami, N.; Ohno, T. *Applied Surface Science* **2012**, *258*, 5803-5809.

(12) Liu, L.; Zhao, H.; Andino, J. M.; Li, Y. *Acs Catalysis* **2012**, *2*, 1817-1828.

(13) Kandiel, T. A.; Robben, L.; Alkaim, A.; Bahnemann, D. *Photochemical & Photobiological Sciences* **2013**, *12*, 602-609.

(14) Li, Z.; Cong, S.; Xu, Y. *Acs Catalysis* **2014**, *4*, 3273-3280.

(15) Ohno, T.; Higo, T.; Saito, H.; Yuajn, S.; Jin, Z.; Yang, Y.; Tsubota, T. *J. Mol. Catal. A: Chem.* **2015**, *396*, 261-267.

(16) Kogo, A.; Sanehira, Y.; Ikegami, M.; Miyasaka, T. *Chem. Lett.* **2016**, *45*, 143-145.

(17) Bahnemann, D.; Henglein, A.; Lilie, J.; Spanhel, L. *J. Phys. Chem.* **1984**, *88*, 709-711.

(18) Bahnemann, D. W.; Hilgendorff, M.; Memming, R. *J. Phys. Chem. B* **1997**, *101*, 4265-4275.

(19) Yoshihara, T.; Katoh, R.; Furube, A.; Tamaki, Y.; Murai, M.; Hara, K.; Murata, S.; Arakawa, H.; Tachiya, M. *J. Phys. Chem. B* **2004**, *108*, 3817-3823.

(20) Meekins, B. H.; Kamat, P. V. *J. Phys. Chem. Lett.* **2011**, *2*, 2304-2310.

(21) Wang, X. L.; Kafizas, A.; Li, X. O.; Moniz, S. J. A.; Reardon, P. J. T.; Tang, J. W.; Parkin, I. P.; Durrant, J. R. *J. Phys. Chem. C* **2015**, *119*, 10439-10447.

(22) Yamakata, A.; Ishibashi, T.; Onishi, H. *Chem. Phys. Lett.* **2001**, *333*, 271-277.

(23) Yamakata, A.; Ishibashi, T.; Onishi, H. *J. Phys. Chem. B* **2001**, *105*, 7258-7262.

(24) Yamakata, A.; Vequizo, J. J. M.; Matsunaga, H. *J. Phys. Chem. C* **2015**, *119*, 24538-24545.

(25) Xu, M. C.; Gao, Y. K.; Moreno, E. M.; Kunst, M.; Muhler, M.; Wang, Y. M.; Idriss, H.; Woll, C. *Phys. Rev. Lett.* **2011**, *106*, 4.

(26) Luttrell, T.; Halpegamage, S.; Tao, J.; Kramer, A.; Sutter, E.; Batzill, M. *Scientific Reports* **2014**, *4*, 1-8.

(27) Yamakata, A.; Kawaguchi, M.; Nishimura, N.; Minegishi, T.; Kubota, J.; Domen, K. *J. Phys. Chem. C* **2014**, *118*, 23897-23906.

(28) Yamakata, A.; Ishibashi, T.; Onishi, H. *J. Phys. Chem. B* **2002**, *106*, 9122-9125.

(29) Yamakata, A.; Yeilin, H.; Kawaguchi, M.; Hisatomi, T.; Kubota, J.; Sakata, Y.; Domen, K. *J. Photochem. Photobiol. A-Chem.* **2015**, *313*, 168-175.

(30) Yamakata, A.; Vequizo, J. J. M.; Kawaguchi, M. *J. Phys. Chem. C* **2015**, *119*, 1880-1885.

(31) Wang, X.; Feng, Z.; Shi, J.; Jia, G.; Shen, S.; Zhou, J.; Li, C. *Phys. Chem. Chem. Phys.* **2010**, *12*, 7083-7090.

(32) Yamada, Y.; Kanemitsu, Y. *Phys. Rev. B* **2010**, *82*.

(33) Knorr, F. J.; Mercado, C. C.; McHale, J. L. *J. Phys. Chem. C* **2008**, *112*, 12786-12794.

(34) Mercado, C. C.; Knorr, F. J.; McHale, J. L.; Usmani, S. M.; Ichimura, A. S.; Saraf, L. V. *J. Phys. Chem. C* **2012**, *116*, 10796-10804.

(35) Bellardita, M.; Di Paola, A.; Palmisano, L.; Parrino, F.; Buscarino, G.; Amadelli, R. *Appl. Catal., B* **2011**, *104*, 291-299.

(36) Na-Phattalung, S.; Smith, M. F.; Kim, K.; Du, M. H.; Wei, S. H.; Zhang, S. B.; Limpijumnong, S. *Phys. Rev. B* **2006**, *73*, 6.

(37) Mattioli, G.; Filippone, F.; Alippi, P.; Bonapasta, A. A. *Phys. Rev. B* **2008**, *78*, 4.

(38) Spreafico, C.; VandeVondele, J. *Phys. Chem. Chem. Phys.* **2014**, *16*, 26144-26152.